


Two coordination polymers: Crystal structures, prevention and nursing values on postoperative infection

Progress in Reaction Kinetics and Mechanism
Volume 47: 1–10
© The Author(s) 2022
Article reuse guidelines:
sagepub.com/journals-permissions
DOI: 10.1177/14686783221090376
journals.sagepub.com/home/prk


Meng Ding¹, Fan Yang^{2,#}, Qingquan Lv³ and Qiongfang Liu⁴

Abstract

In this current work, two fresh transition metal coordination polymers (CPs) have been created with the reaction between terphenyl-3,3'',5,5''-tetracarboxylic acid (H₄L), the symmetrical rigid carboxylic acid ligand and the relevant metal salts under the reaction conditions of solvothermal, and the chemical compositions of the compounds respectively are {[Cu₂(TPTC) (DMF)₂(H₂O)]·2DMF·2H₂O} (2) and {[Zn (TPTC) (1,2-bimb)₂]·4(H₂O)}_n (1, bimb = 1,2-bis((1H-imidazol-1-yl)methyl)benzene). Moreover, the prevention and nursing values of the compound on postoperative infection was explored and their corresponding mechanism also was investigated. Firstly, enzyme linked immunosorbent assay kit (ELISA) was employed to detect the release of inflammatory cytokines into plasma. Additionally, the expression of the bacterial survival genes was determined via exploiting the real time reverse transcription-polymerase chain reaction (RT-PCR) after treated with the compound.

Keywords

Coordination complex, postoperative infection, inflammatory cytokines

¹Operating Room, Hankou Hospital of Wuhan City, Wuhan, China

²Anesthesia Department, Hankou Hospital of Wuhan City, Wuhan, China

³Medical Department, Hankou Hospital of Wuhan City, Wuhan, China

⁴Hospital Infection Management Department, Hankou Hospital of Wuhan City, Wuhan, China

#Meng Ding and Fan Yang contribute equal to this article as co-first author

Corresponding author:

Meng Ding, Operating Room, Hankou Hospital of Wuhan City, Wuhan 430012, China.

Email: m_d123@163.com

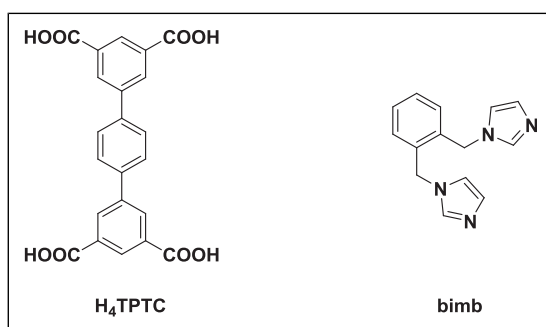


Creative Commons Non Commercial CC BY-NC: This article is distributed under the terms of the Creative Commons Attribution-NonCommercial 4.0 License (<https://creativecommons.org/licenses/by-nc/4.0/>) which permits non-commercial use, reproduction and distribution of the work without further permission provided the original work is attributed as specified on the SAGE and Open Access pages (<https://us.sagepub.com/en-us/nam/open-access-at-sage>).

Introduction

Postoperative infection is an important form of infection after surgery, which seriously affects the recovery progress of patients after surgery.¹ A large amount of data shows that surgical incision infections account for more than 10% of nosocomial infections, which seriously affects the quality of medical services and the recovery of patients.² As a result, in the current work, the novel candidates were designed and synthesized and their biological application values were evaluated.

In recent several years, the transition metal complexes involving organic ligands and inorganic metal ions are the focus of recent research on account of their versatility in structure and their extensive applications range for instance the antibacterial and antitumor activities, the performances of luminescence, catalytic activities, the adsorption of gas, DNA binding, and magnetic performances.³⁻⁶ As is known to all, for the metal-organic complexes, the diversity in structure and activity performances are decided by the selection of metal atoms and organic ligands applied to a great extent, together with the reaction mechanism for acquiring the complex.⁷⁻¹¹ As a result, the choice of appropriate metal ions and the rational design of organic ligands possess a significant function in acquiring the complexes having ideal performances.¹²⁻¹⁵ The terphenyl-3,3'',5,5''-tetracarboxylic acid (H_4TPTC) was employed in our investigation on the basis of these reasons: (1) the rigid skeleton for the ligand of H_4TPTC is helpful to establish the stable CPs. (2) the carboxyl groups of CPs can be coordinated in many ways, which makes it possible to establish the CPs having outstanding performances and fresh architectures, and (3) the conjugated aromatic rings of CPs are conducive to electron transport and the interactions of π - π with the bioactivity molecules, which might endow them with interesting bioactivity.¹⁶⁻²⁰ In this current work, two fresh transition metal coordination polymers (CPs) have been created with the reaction between terphenyl-3,3'',5,5''-tetracarboxylic acid (H_4L , Scheme 1), the symmetrical rigid carboxylic acid ligand and the relevant metal salts under the reaction conditions of solvothermal, and the chemical compositions of the compounds respectively are $\{[Cu_2(TPTC)(DMF)_2(H_2O)] \cdot 2DMF \cdot 2H_2O\}$ (2) and $\{[Zn(TPTC)(1,2-bimb)_2] \cdot 4(H_2O)\}_n$ (1). After providing the novel compounds having new architecture, their prevention and nursing values on postoperative infection was explored and the related mechanism was discussed as well.



Scheme 1. The chemical drawings for the organic ligands.

Experimental

Chemicals and measurements

All of the starting chemicals employed in our investigation could be acquired from the market, and they were exploited without processing. The FT-IR spectra could be performed utilizing KBr pellets and it was recorded through employing the spectrometer of Nicolet Impact 750 FTIR with the infrared spectra region from 400 cm^{-1} to 4000 cm^{-1} . Through utilizing the analyzer of Perkin-Elmer 2400C, the analysis of Hydrogen, Nitrogen and Carbon elements was implemented.

Preparation and characterization for $\{[\text{Zn}(\text{TPTC})(1,2\text{-bimb})_2]\cdot 4(\text{H}_2\text{O})\}_n$ (1) and $\{[\text{Cu}_2(\text{TPTC})(\text{DMF})_2(\text{H}_2\text{O})]\cdot 2\text{DMF}\cdot 2\text{H}_2\text{O}\}$ (2)

2.1 mg and 0.005 mmol of H_4TPTC , 0.010 mmol and 2.4 mg of 1,2-bimb and 15 mg and 0.05 mmol of $\text{Zn}(\text{NO}_3)_2\cdot 6\text{H}_2\text{O}$ were dissolved into the mixed solution of CH_3CN and H_2O (4 mL, with 1:1 volume ratio). The product was kept in the reaction vessel and then it was heated for 72 hours to 130°C . The colorless needle crystals can be acquired after dropping to the environmental temperature slowly. (with 35% yield on the basis of Zn). Elemental analysis (%): calcd for the $\text{C}_{50}\text{H}_{47}\text{Zn}_2\text{N}_8\text{O}_{12}$: N, 10.35%, C, 55.47% and H, 4.38%. Found: N, 10.68, C, 55.95 and H, 4.24%. IR (KBr pallet, cm^{-1}): 3354 (s), 2836 (m), 1600 (s), 1551 (s), 1506 (m), 1490 (m), 1455 (s), 1433 (m), 1386 (m), 1366 (m), 1337 (s), 1312 (s), 1180 (w), 1149 (m), 1108 (s), 1008 (w), 947 (w), 907 (w), 843 (m), 769 (m), 737 (m), 707 (m), 687 (m), 613 (w), 598 (w), 562 (w), and 491 (m).

The mixture synthesized from 0.1 mmol and 0.025 g of terphenyl-3,3'',5,5''-tetracarboxylic acid, 0.048 g and 0.2 mmol of $\text{Cu}(\text{NO}_3)_2\cdot 3\text{H}_2\text{O}$ and 3 mL of DMF was stirred in the air for half an hour. The obtaining product was kept in the vial container (25 mL) and then this solution was heated for 3 days to 105°C . Subsequently, the mixture of reaction was dropped at 2°C h^{-1} rate to environmental temperature. The complex 2's blue massive crystals were gained with the yield of 32% according to zinc. Elemental analysis results calculated for the $\text{C}_{34}\text{H}_{44}\text{Cu}_2\text{N}_4\text{O}_{15}$ (1): N, 6.40%, C, 46.63% and H, 5.06%; found: N, 6.58, C, 46.01 and H, 5.50%. IR (KBr pallet, cm^{-1}): 3423 (m), 3063 (m), 2934 (m), 2783 (m), 1593 (s), 1563 (s), 1489 (s), 1451 (s), 1380 (m), 1364 (m), 1338 (s), 1312 (s), 1233 (s), 1162 (m), 1150 (m), 1108 (s), 1026 (m), 1005 (w), 925 (s), 836 (m), 776 (s), 756 (s), 710 (m), 689 (s), 618 (w), 580 (w), and 535 (s).

The data for X-ray can be analyzed through SuperNova diffractometer. For the strength data, it was analyzed via exploiting the CrysAlisPro, and this data was then converted to HKL files. And, the original structural manners were established by the direct means based SHELXS, and after that, least-squares method based SHELXL-2014 was exploited to modify. The anisotropic parameters were mixed with global non-hydrogen atoms. Next, the entire hydrogen atoms were geometrically fixed via applying the AFIX commands to carbon atoms that they adjacent to. The compounds' details of optimization and their parameters of crystallography were revealed in length in the [Table 1](#).

Inflammatory cytokines determination

After the establishment of model and the treatment of compound, the inflammatory cytokines releasing into plasma in diverse groups was determined by utilizing the ELISA detection kit. This implementation was completed fully in accordance with the protocols of manufactures with minor change. Afterward, 40 BALB/c mice applied in this work were provided via the Shanghai Southern Model Biotechnology Co, Ltd and in this research, all of the conduction were granted through the

Table I. The complexes' details of optimization and their parameters of crystallography.

Identification code	1	2
Empirical formula	C ₅₀ H ₃₈ N ₈ O ₈ Zn ₂	C ₂₈ H ₂₆ Cu ₂ N ₂ O ₁₁
Formula weight	1009.62	693.59
Temperature/K	296.15	296.15
Crystal system	Monoclinic	Monoclinic
Space group	P2 ₁ /n	P2 ₁
a/Å	9.963 (2)	9.6236 (11)
b/Å	15.6741 (10)	16.518 (3)
c/Å	31.559 (3)	15.265 (2)
α/°	90	90
β/°	92.782 (2)	107.3170 (10)
γ/°	90	90
Volume/Å ³	4922.6 (11)	2316.6 (6)
Z	4	2
ρ _{calc} /cm ³	1.362	0.994
μ/mm ⁻¹	1.035	0.958
Data/restraints/parameters	9330/36/613	11040/1/393
Goodness-of-fit on F ²	0.971	0.947
Final R indexes [$I \geq 2\sigma(I)$]	R ₁ = 0.0633, ωR ₂ = 0.1387	R ₁ = 0.0619, ωR ₂ = 0.1543
Final R indexes [all data]	R ₁ = 0.1449, ωR ₂ = 0.1697	R ₁ = 0.1113, ωR ₂ = 0.1799
Largest diff. peak/hole/e Å ⁻³	1.11/-0.66	1.22/-0.61
CCDC	2,078,175	2,078,176

Animal Ethics Committee of China. The *Staphylococcus aureus* was used to infect the animal to induce the postoperative infection. Then, the treatment was completed via utilizing the compounds with 5 mg/kg. The animal plasma was collected and the inflammatory cytokines content was detected.

Bacterial survival genes expression

The real time RT-PCR was further accomplished in the current investigation for the detection of the bacterial survival genes expression after the incubation of compound. This study was implemented strictly in the light of instructions with minor modifications. Shortly, the *S. aureus* were harvested and then they were inoculated into plates of 96 well, and the treatment was conducted after adding the compounds at 10 ng/mL, 20 ng/mL and 50 ng/mL concentration. Next, the *S. aureus* were harvested and in cells, the overall RNA could be extracted through utilizing the reagent of TRIZOL. After the determination of the entire RNA concentration, the concentration was reverse transcript into the cDNA. In the end, the real time RT-PCR was performed and the *S. aureus* survival genes relative expression was detected.

Results and discussion

Crystal structures

In accordance with the analysis of the diffraction of X-ray, the complex **1** is part of the space group P2₁/n of monoclinic system. As can be found from the [Figure 1\(a\)](#), in its asymmetric unit, there exist

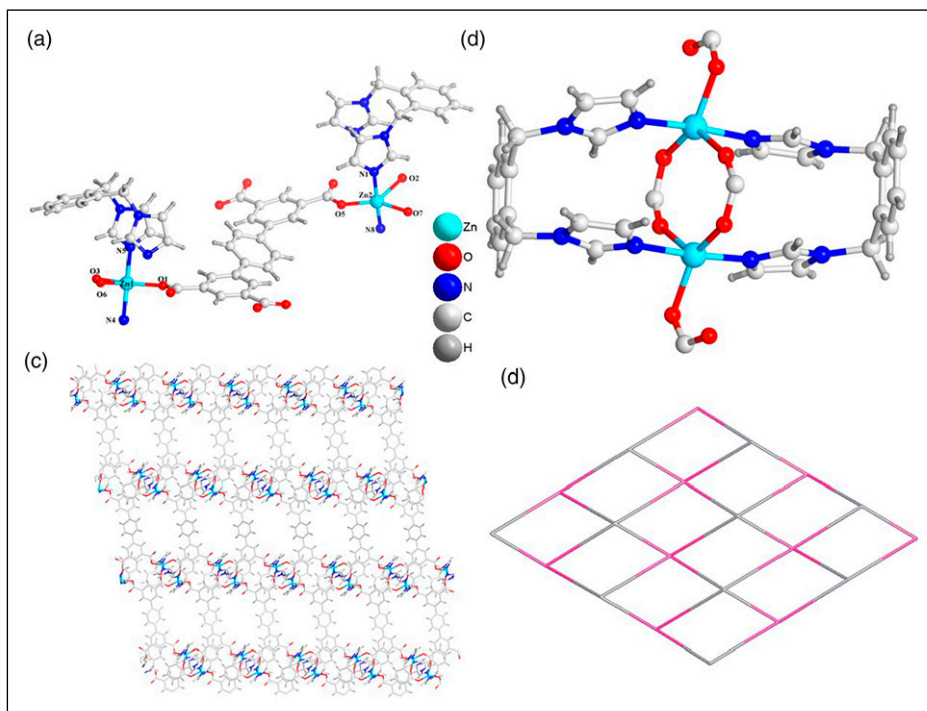


Figure 1. (a) The asymmetry unit for the compound **1**. (b) The SBU of [Zn₂(COO)₄] in complex **1**. (c) The **1**'s two-dimensional layered architecture. (d) The **1**'s four-linked **sql** net.

2 Zn(II) ions, 2 connectors of 1,2-bimb, along with a TPTC⁴⁻ connector. The Zn1 ion and the Zn2ⁱⁱ ion exhibit the same surrounding of coordination. The Zn1 is connected through 2 nitrogen-atoms (N4ⁱⁱ and N5, respectively) in 2 distinct connectors of 1,2-bimb and 3 oxygen-atoms (namely, O6ⁱⁱ, O3ⁱ, and O1) derived from 3 diverse connectors of TPTC⁴⁻ to producing a triangular biconical geometry. The separations of Zn–O/N are between 1.964 (3) Å and 2.287 (4) Å, and the angles of O–Zn–N/O are between 85.56 (13) ° and 174.98 (18) °. The consecutive Zn1 ion and the Zn2ⁱⁱ ion are linked to 2 carboxyl groups in order to create the binuclear SBUs of [Zn₂(COO)₄] (Figure 1(b)), which are connected through the TPTC⁴⁻ connector and 1,2-bimb connector by using the bonding pattern of $\mu_6\text{-}\eta^1\text{:}\eta^1\text{:}\eta^1\text{:}\eta^1\text{:}\eta^1\text{:}\eta^1$ to establish a two-dimensional architecture (Figure 1(c)). Topologically, when both SBUs of [Zn₂(COO)₄] and the ligands of TPTC⁴⁻ can be applied as the four-linked nodes, the complex **1** have topology type of **sql** (Figure 1(d)).

The complex **2**'s structure is constructed from 2 distinctive Cu(II) ions, a distinctive connector of TPTC⁴⁻, and 2 coordinated molecules of DMF as well as a coordinated molecule of water (Figure 2(a)). The metal ions are linked through the connector of TPTC⁴⁻ in order to generate the binuclear cluster, and the 2 metals connected via 3 TPTC⁴⁻ connector carboxylic acid groups. The 4 TPTC⁴⁻ connector carboxylic acid groups employ 3 diverse coordination patterns, i.e. bridging bidentate, chelating bidentate along with μ_3 -chelating–bridging tridentate, so as to coordinate to 7 copper atoms (Figure 2(b)). For the Cu1 ion, its coordination sphere is accomplished via the coordination of a coordinated molecule of water and 2 molecules of DMF, and for the Cu2 ion, its coordination sphere is accomplished via the chelation of another connector of TPTC⁴⁻ carboxylic acid. Therefore, each of the binuclear cluster is coordinated with 4 connectors of TPTC⁴⁻; each of the

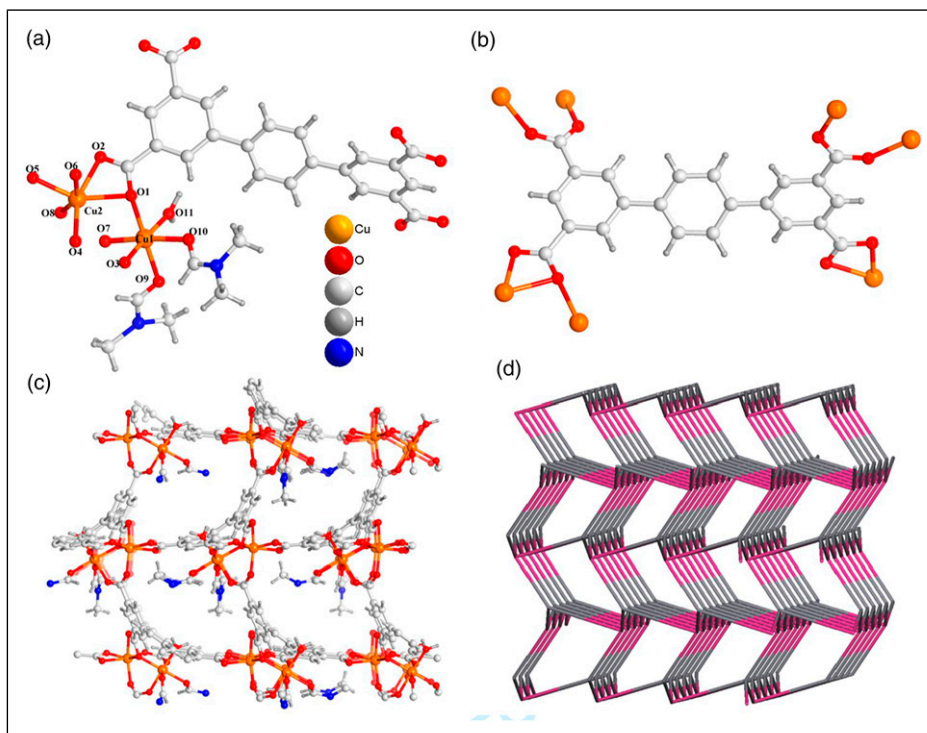


Figure 2. (a) The asymmetry unit for the complex **2**. (b) The coordination manners for carboxylic acid ligand in compound **2**. (c) The **2**'s three-dimensional net (d) The **2**'s four-linked lonsdaleite (**lon**) topology.

ligand coordinates with 4 binuclear clusters in turn. As a result, each of the binuclear cluster is bound with 4 ligands. Each of the ligand is bonded with 4 clusters of Cu₂ in tune. The molecular building blocks (MBBs) of {Cu₂(CO₂)₅} was combined with four-linked ligands with a ratio of 1:1 to generate a three-dimensional skeleton, which displayed the elliptical channels (atom-to-atom separations) with the size of 11.5 × 14.8 Å² along plane ab (Figure 2(c)). In topology, as a result, the binuclear metal cluster and each of the ligand apply as the four-linking nodes to form a global three-dimensional net containing an uninodal four-linked lonsdaleite (**lon**) topology (Figure 2(d)). On the basis of PLATON calculation, the effective free volume is approximately 68.3%.

To check the phase purity of the products, powder X-ray diffraction (PXRD) experiments have been carried out for these complexes (Figure 3(a) and (b)). The peak positions of the experimental and simulated PXRD patterns are in good agreement with each other, indicating that the crystal structures are truly representative of the bulk crystal products. The differences in intensity may be owing to the preferred orientation of the crystal samples.

Compound significantly inhibited the releasing of the inflammatory cytokines into the plasma

The compounds **1** and **2** were synthesized in this research for the postoperative infection treatment. Because, they was generally combined with the enhanced inflammatory response level during the postoperative infection, exhibited as the enhanced inflammatory cytokines releasing levels. As a

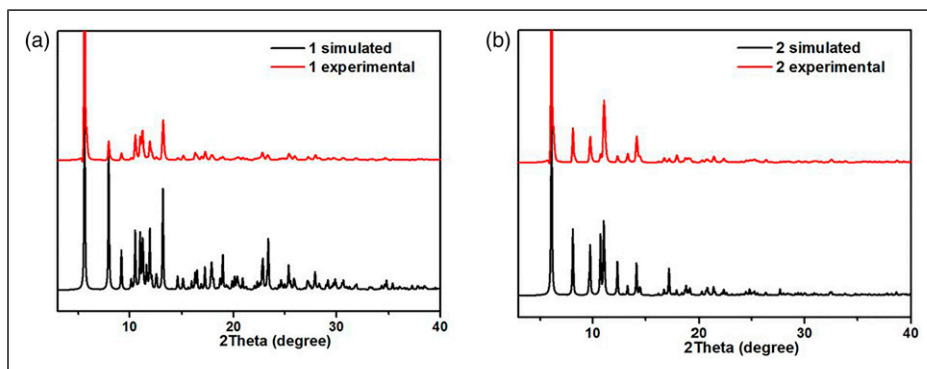


Figure 3. The PXRD patterns for complex 1 (a) and complex 2 (b).

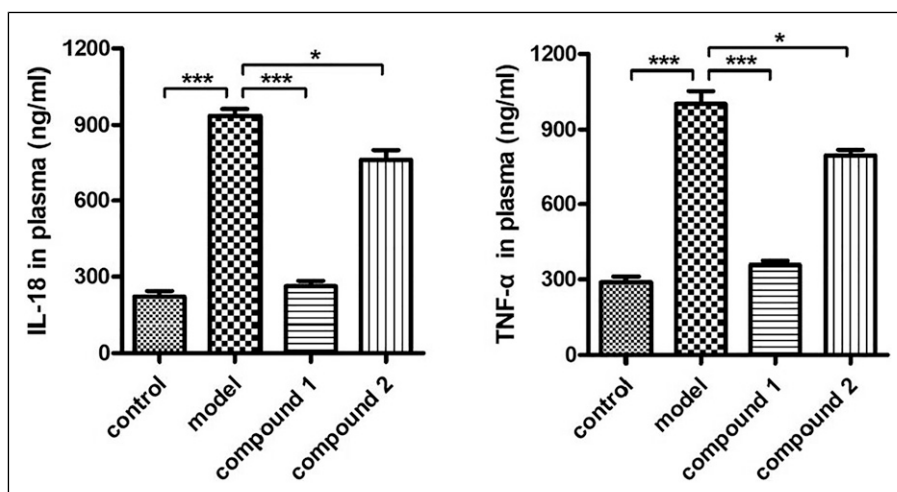


Figure 4. Significantly inhibited inflammatory cytokines releasing into plasma after treating with the compound. The *Staphylococcus aureus* was used to infect the animal to induce the postoperative infection. Then, the treatment was completed by utilizing the compounds with 5 mg/kg. The animal plasma was harvested and the inflammatory cytokines content was determined.

result, the ELISA detection kit was performed and the inflammatory cytokines content released into plasma was detected. The outcomes in the Figure 4 exhibited that the model group has a much higher inflammatory cytokines in comparison with control group, with the value of <0.005 . After treated with the compound 1, the inflammatory cytokines released into plasma was remarkably decreased. The complex 2's inhibitory influence was much weaker than compound 1.

Compound obviously reduced the expression of the bacterial survival genes

As previous described, the 1 was more superior than that of the 2 on the inhibition of the inflammatory cytokines releasing into the plasma. In addition to this, the influence of the new compounds on the bacterial survival genes expression was still required to be explored. As the

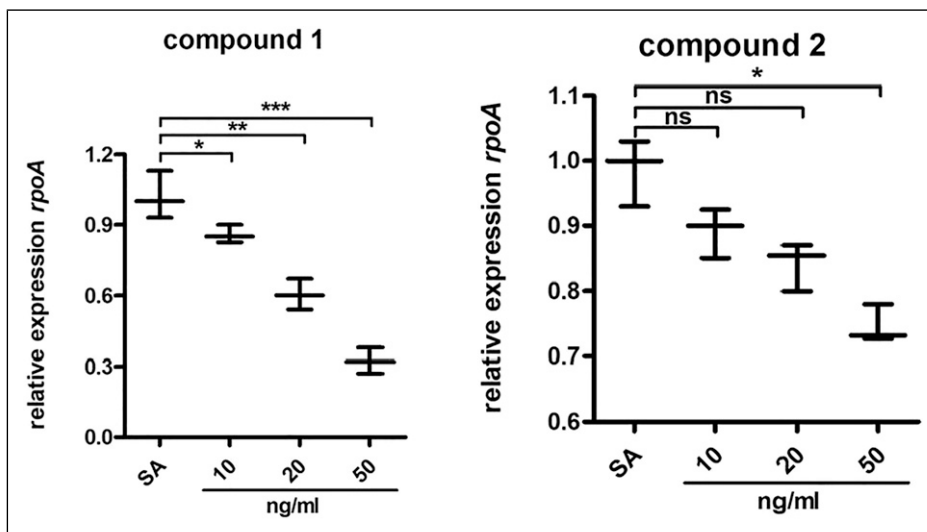


Figure 5. Obviously reduced expression of the bacterial survival genes after compound treatment. The *Staphylococcus aureus* were collected and incubated with compounds **1** and **2** with different concentrations. The real time RT-PCR was conducted and the expression of the bacterial survival genes was determined.

results illustrated in the Figure 5, the bacterial survival genes expression was much reduced by compound **1** with a dose dependent manner. Different from compound **1**, compound **2** exhibited a much weaker influence on the expression of the bacterial survival genes

Conclusion

On the whole, we have produced two fresh transition metal coordination polymers triumphantly with the reaction between terphenyl-3,3',5,5'-tetracarboxylic acid (H_4L), the symmetrical rigid carboxylic acid ligand and the relevant metal salts under the reaction conditions of solvothermal. The analysis of structure suggest that the **1** is a four-linked two-dimensional nets with **sql** type of topology, and the compound **2** reveals a three-dimensional uninodal four-linked lonsdaleite (**lon**) topology on the basis of the binuclear copper clusters. The ELISA assay results exhibited that the **1** was more superior than that of the complex **2** on the inhibition of the inflammatory cytokines releasing into the plasma. Besides, the expression of the bacterial survival genes was also inhibited via the complex **1**, and this much stronger in contrast to the **2**. In the end, we gained the summary that the **1** may become an outstanding candidate for the treatment of postoperative infection via the inhibition of inflammatory response and the reduction of the bacterial survival genes expression.

Declaration of conflicting interests

The author(s) declared no potential conflicts of interest with respect to the research, authorship, and/or publication of this article.

Funding

The author(s) received no financial support for the research, authorship, and/or publication of this article.

References

1. Goswami K, Stevenson KL and Parvizi J. Intraoperative and postoperative infection prevention. *The J Arthroplasty* 2020; 35: S2–S8.
2. Vieira ALG, Stocco JGD, Ribeiro ACG, et al. Dressings used to prevent surgical site infection in the postoperative period of cardiac surgery: integrative review. *Rev Esc Enferm USP* 2018; 52: e03393.
3. Bharati AK, SomnathLama P, Lama P, et al. A novel mixed ligand Zn-coordination polymer: synthesis, crystal structure, thermogravimetric analysis and photoluminescent properties. *Inorg Chim Acta* 2020; 500: 119219.
4. Fan L, Zhao D, Li B, et al. An exceptionally stable luminescent cadmium(ii) metal-organic framework as a dual-functional chemosensor for detecting Cr(vi) anions and nitro-containing antibiotics in aqueous media. *CrystEngComm* 2021; 23: 1218–1225.
5. Wang F, Tian F, Deng Y, et al. Cluster-based multifunctional copper(II) organic framework as a photocatalyst in the degradation of organic dye and as an electrocatalyst for overall water splitting. *Cryst Growth Des* 2021; 21: 4242–4248.
6. Ran H, Du H, Ma C, et al. Effects of A/B-Site Co-doping on microstructure and dielectric thermal stability of AgNbO₃ ceramics. *Sci Adv Mater* 2021; 13: 741–747.
7. Kang L, Du H, Deng J, et al. Synthesis and catalytic performance of a new V-doped CeO₂-supported Alkali-activated-steel-slag-based photocatalyst. *J Wuhan Univ Technology-Mater. Sci. Ed.* 2021; 36: 209–214.
8. Feng X, Feng Y-Q, Liu L, et al. A series of Zn-4f heterometallic coordination polymers and a zinc complex containing a flexible mixed donor dicarboxylate ligand. *Dalton Trans* 2013; 42: 7741–7754.
9. Hu M-L, Razavi SAA, Piroozzadeh M, et al. Sensing organic analytes by metal-organic frameworks: a new way of considering the topic. *Inorg Chem Front* 2020; 7: 1598–1632.
10. Hu M-L, Safarifard V, Doustkhah E, et al. Taking organic reactions over metal-organic frameworks as heterogeneous catalysis. *Microporous Mesoporous Mater* 2018; 256: 111–127.
11. Wang X-L, Xiong Y, Liu X-X, et al. Four new Zn(II)-coordination polymers based on a bi-methylene-bridged pyridyl-amide and various polycarboxylates and their luminescence property. *Polyhedron* 2018; 151: 264–272.
12. Mu B, Li F and Walton KS. A novel metal-organic coordination polymer for selective adsorption of CO₂ over CH₄. *Chem Commun* 2009; 47: 2493–2495.
13. Mukherjee S, Ganguly S, Manna K, et al. Green approach to synthesize crystalline nanoscale ZnII-coordination polymers: cell growth inhibition and immunofluorescence study. *Inorg Chem* 2018; 57: 4050–4060.
14. Bai N, Gao R, Wang H, et al. Five transition metal coordination polymers driven by a semirigid trifunctional nicotinic acid ligand: selective adsorption and magnetic properties. *CrystEngComm* 2018; 20: 5726–5734.
15. Xiao Q-Q, Dong G-Y, Li Y-H, et al. Cobalt(II)-based 3D coordination polymer with unusual 4,4,4-connected topology as a dual-responsive fluorescent chemosensor for acetylacetone and Cr₂O₇²⁻. *Inorg Chem* 2019; 58: 15696–15699.
16. Wen T, Zhang D-X, Liu J, et al. A multifunctional helical Cu(i) coordination polymer with mechano-chromic, sensing and photocatalytic properties. *Chem Commun* 2013; 49: 5660–5662.
17. Han Z, Yu Y, Zhang Y, et al. Al-coordination polymer-derived nanoporous nitrogen-doped carbon microfibers as metal-free catalysts for oxygen electroreduction and acetalization reactions. *J Mater Chem A* 2015; 3: 23716–23724.
18. Ren Y-N, Xu W, Zhou L-X, et al. Efficient tetracycline adsorption and photocatalytic degradation of rhodamine B by uranyl coordination polymer. *J Solid State Chem* 2017; 251: 105–112.

19. Seco JM, Oyarzabal I, Pérez-Yáñez S, et al. Designing multifunctional 5-Cyanoisophthalate-based coordination polymers as single-molecule magnets, adsorbents, and luminescent materials. *Inorg Chem* 2016; 55: 11230–11248.
20. Zhao Y-M, Tang G-M, Wang Y-T, et al. Copper-based metal coordination complexes with Voriconazole ligand: syntheses, structures and antimicrobial properties. *J Solid State Chem* 2018; 259: 19–27.